OXFORD
SOT | Society of Toxicology
www.toxsci.oxfordjournals.org

TOXICOLOGICAL SCIENCES, 141(1), 2014, 244–253

doi: 10.1093/toxsci/kfu122
Advance Access Publication Date: June 27, 2014

Different Dose-Dependent Mechanisms Are Involved in Early Cyclosporine A-Induced Cholestatic Effects in HepaRG Cells

Ahmad Sharanek*,†, Pamela Bachour-El Azzi*,†, Houssein Al-Attrache*,†, Camille C. Savary*,†, Lydie Humbert‡, Dominique Rainteau‡, Christiane Guguen-Guillouzo*,†, and André Guillouzo*,†,1

*Inserm UMR991, Foie, Métabolisme et Cancer, Rennes, France, †Université de Rennes 1, Rennes, France and ‡ERL Inserm U1157/UMR7203, Faculté de Medecine Pierre et Marie Curie, Site Saint Antoine, Paris, France

[1]To whom correspondence should be addressed. Fax: +33223235385. E-mail: andre.guillouzo@univ-rennes1.fr.

ABSTRACT

Mechanisms involved in drug-induced cholestasis in humans remain poorly understood. Although cyclosporine A (CsA) and tacrolimus (FK506) share similar immunosuppressive properties, only CsA is known to cause dose-dependent cholestasis. Here, we have investigated the mechanisms implicated in early cholestatic effects of CsA using the differentiated human HepaRG cell line. Inhibition of efflux and uptake of taurocholate was evidenced as early as 15 min and 1 h respectively after addition of 10μM CsA; it peaked at around 2 h and was reversible. These early effects were associated with generation of oxidative stress and deregulation of cPKC pathway. At higher CsA concentrations (≥50μM) alterations of efflux and uptake activities were enhanced and became irreversible, pericanalicular F-actin microfilaments were disorganized and bile canaliculi were constricted. These changes were associated with induction of endoplasmic reticulum stress that preceded generation of oxidative stress. Concentration-dependent changes were observed on total bile acid disposition, which were characterized by an increase and a decrease in culture medium and cells, respectively, after a 24-h treatment with CsA. Accordingly, genes encoding hepatobiliary transporters and bile acid synthesis enzymes were differently deregulated depending on CsA concentration. By contrast, FK506 induced limited effects only at 25–50μM and did not alter bile canaliculi. Our data demonstrate involvement of different concentration-dependent mechanisms in CsA-induced cholestasis and point out a critical role of endoplasmic reticulum stress in the occurrence of the major cholestatic features.

Key words: oxidative stress; endoplasmic reticulum stress; cPKC signaling; hepatocytes; bile acids; transporters; tacrolimus

ABBREVIATIONS

CsA	cyclosporine A
FK506	tacrolimus
cPKC	classical protein kinase c
ADR	adverse drug reaction
DILI	drug-induced liver injury
BSEP	bile salt export pump
E17G	estradiol 17ß-D-glucuronide
MRP2	multidrug resistance-associated protein 2
MDR1	multidrug resistance 1
ER	endoplasmic reticulum
MTT	methylthiazoletetrazolium
DMSO	dimethyl sulfoxide
RNA	ribonucleic acid
RT-qPCR	real-time quantitative polymerase chain reaction
NTCP	Na^+-dependent taurocholate cotransporting polypeptide
TA	taurocholic acid
ROS	reactive oxygen species
H2-DCFDA	2',7'-dichlorodihydrofluorescein
NAC	N-acetyl-cysteine

Nrf2	NF-E2-related factor 2
HO1	heme oxygenase 1
MnSOD	manganese superoxide dismutase
ATF4	activating transcription factor 4
ATF6	activating transcription factor 6
GRP78	glucose regulated protein,78KD
CHOP	C/Ebp-homologous protein
PBA	4-phenyl butyric acid
CDF	5(6)-carboxy-2′,7′-dichlorofluorescein diacetate
BA	bile acids
H7	1-(5-isoquinolinylsulfonyl)-2-methyl-piperazine
CAR	constitutive androstane receptor
PXR	pregnane X receptor
FXR	farnesoid X receptor
BCRP	breast cancer resistance protein
MDR3	multidrug resistance 3
MRP3	multidrug resistance-associated protein 3
MRP4	multidrug resistance-associated protein 4
CYP7A1	cytochrome P450 7A1
CYP8B1	cytochrome P450 8B1
CYP27A1	cytochrome P450 27A1
CYP3A4	cytochrome P450 3A4

Adverse drug reactions (ADRs) are usually classified as either dose-dependent and reproducible (intrinsic) or unpredictable (idiosyncratic) occurring only in certain susceptible patients and being not overtly dose-dependent (Park *et al.*, 2005). Many different classes of marketed drugs and herbals have been reported to cause drug-induced liver injury (DILI) in humans, accounting for more than 50% of cases of acute liver failure in the United States (Lee, 2003). DILI encompasses a large spectrum of lesions, including apoptosis/necrosis, phospholipidosis, steatosis, and cholestasis.

Intra-hepatic cholestasis represents a frequent manifestation of DILI in humans (Lee, 2003). In many cases, it results from alterations of the hepatobiliary transporter system, in particular the bile salt export pump (BSEP), which is the most physiologically important canalicular bile transporter (Stieger *et al.*, 2007). Other disturbances, such as altered cell polarity, disruption of cell-to-cell junctions, and cytoskeleton disorganization, can also participate in cholestasis. The mechanisms by which drugs induce cholestasis are diverse and remain poorly understood (Anthérieu *et al.*, 2013). Intracellular signaling has emerged as a fundamental mechanism to explain the development of different models of cholestasis (Crocenzi *et al.*, 2004); thus, the Ca^{2+}-dependent PKC isoforms (cPKC) have been demonstrated to be involved in estradiol 17ß-D-glucuronide (E17G)- and tert-butylhydroperoxide-induced cholestasis (Barosso *et al.*, 2012; Pérez *et al.*, 2006). A role for oxidative stress as a primary causal agent and/or an aggravating factor has been evidenced in extrahepatic and intrahepatic cholestasis (Anthérieu *et al.*, 2013; Pérez *et al.*, 2006; Roma and Pozzi, 2008).

Cyclosporine A (CsA) is well recognized as a dose-dependent cholestatic inducing agent. It has been shown to alter bile secretion in *in vitro* (Princen *et al.*, 1991) and short-term *in vivo* studies (Mizuta *et al.*, 1999). CsA also acts as a competitive inhibitor of BSEP, MRP2, and MDR1 and caused disorganization of pericanalicular F-actin cytoskeleton (Román and Coleman, 1994). CsA disturbs the endoplasmic reticulum (ER)-Golgi transport by altering vesicle-mediated transport (Sarró *et al.*, 2012). By contrast, tacrolimus (FK506), another immunosuppressant that possesses similar immunosuppressive properties as CsA (Tocci *et al.*, 1989), has usually no effect even at supra-therapeutic concentrations in humans. The reasons why the liver is so differently sensitive to the two immunosuppressant agents remain unclear.

In the present study, we have investigated early effects of CsA and FK506 in the metabolically competent human HepaRG cells. In addition to phases I and II metabolizing enzymes (Aninat *et al.*, 2006), these cells exhibit functional sinusoidal and canalicular transporters and are now largely used for studying both acute and chronic effects of xenobiotics in human liver (Anthérieu *et al.*, 2012; Guguen-Guillouzo and Guillouzo, 2010). Our data show that unlike FK506, CsA induced early cholestatic effects, involving different dose-dependent mechanisms in HepaRG cells.

MATERIALS AND METHODS

Chemicals. Cyclosporine A (CsA), methylthiazoletetrazolium (MTT), N-acetyl-cysteine (NAC), 4-phenyl butyric acid (PBA), 1-(5-isoquinolinylsulfonyl)-2-methyl-piperazine (H7), and 5(6)-carboxy-2′,7′-dichlorofluorescein diacetate (CDF) were purchased from Sigma (St. Quentin Fallavier, France). Tacrolimus (FK506) was provided by Tocris Bioscience (Bristol, UK), 2',7'-dichlorodihydrofluorescein (H2- DCFDA) was obtained from Invitrogen Molecular Probe (Saint Aubin, France). [^{3}H]-Taurocholic acid ([^{3}H]-TA) was from Perkin Elmer (Boston, MA). The specific antibodies against phospho-p38 MAP kinase and p38 MAP kinase were purchased from Cell Signaling Technology (Beverly, MA). Go¨6976 and SB203580 were from Calbiochem (San Diego, CA). BAPTA/AM was obtained from Alexis Co. (Nottingham, UK). Phalloidin fluoprobe SR101 (200 U/ml) was purchased from Interchim (Montluçon France). Hoechst dye was from Promega (Madison, Wisconsin). Other chemicals were of reagent grade.

Cell cultures. HepaRG cells were seeded at a density of 2.6×10^4 cells/cm^2 in Williams E medium supplemented with 10% fetal bovine serum, 100 IU/ml penicillin, 100 mg/ml streptomycin, 5 mg/ml insulin, 2mM glutamine, and 50mM hydrocortisone hemisuccinate. After 2 weeks, HepaRG cells were shifted to the same medium supplemented with 2% dimethyl sulfoxide (DMSO) for further 2 weeks in order to obtain confluent differentiated cultures with maximum functional activities. At this time, these cultures contained hepatocyte-like and progenitors/primitive biliary-like cells (Cerec *et al.*, 2007).

Cell viability. Cytotoxicity was evaluated by the MTT colorimetric assay. Briefly, cells were seeded in 24-well plates and treated with various concentrations of CsA and FK506. After medium removal, 500 µl serum-free media containing MTT (0.5 mg/ml) were added to each well and incubated for 2 h at 37°C. The water-insoluble formazan was dissolved in 500 µl DMSO and absorbance was measured at 550 nm (Aninat *et al.*, 2006).

Measurement of reactive oxygen species. Reactive oxygen species (ROS) generation was determined by the H2-DCFDA assay. Cells were incubated for 2 h at 37°C with 2µM H2-DCFDA; then they were washed with cold phosphate buffered saline (PBS) and scraped in phosphate buffer (10mM, pH 7.4)/methanol (vol/vol) supplemented with Triton X-100 (0.1%). Fluorescence intensity of cell extracts was determined by spectrofluorimetry using excitation/emission wavelengths of 498/520 nm (Anthérieu *et al.*, 2013).

Real-time quantitative polymerase chain reaction analysis. Total RNA was extracted from 10^6 HepaRG cells with the SV total RNA isolation system (Promega). RNAs were reverse transcribed into cDNA

and real-time quantitative polymerase chain reaction (RT-qPCR) was performed using a SYBR Green mix. Primer sequences are listed in Supporting table 1.

Efflux of taurocholate acid. Cells were first exposed to 43.3nM [^{3}H]-TA for 30 min to induce intracellular accumulation of [^{3}H]-TA, then washed with PBS and incubated with or without CsA or FK506 at different time points (from 0 to 6 h) in a standard buffer with Ca^{2+} and Mg^{2+}. After the incubation time, cells were washed with PBS and incubated for 5 min with Ca^{2+}- and Mg^{2+}-free buffer in order to disrupt canalicular tight junctions. Then, they were scraped in 0.1 N NaOH and the remaining radiolabeled substrate was measured through scintillation counting to determinate TA efflux. To discriminate between basolateral and canalicular efflux, cells were incubated in parallel in either standard or Ca^{2+}- and Mg^{2+}-free buffer for 30 min after TA uptake before measuring the remaining radiolabeled TA. Canalicular efflux was calculated using this equation: Canalicular efflux = Radioactivity in efflux medium Ca^{2+}- and Mg^{2+}-free buffer - Radioactivity in efflux medium standard buffer (Marion *et al.*, 2012).

CDF excretion. After 2 h of exposure to CsA or FK506, cells were incubated with 3μM CDFDA, which is hydrolyzed by intracellular esterases to CDF, a substrate of multidrug resistance-associated protein 2 (MRP2) for 20 min at 37°C and then washed with PBS. Imaging was done using inverted microscope Zeiss Axiovert 200M and AxioCam MRm.

Na+-dependent taurocholic cotransporting polypeptide activity. Activity of the Na+-dependent taurocholic cotransporting polypeptide (NTCP) transporter was estimated through determination of sodium-dependent intracellular accumulation of the radiolabeled [^{3}H]-TA substrate. After treatment with either drug, cells were incubated with 43.3nM of radio-labeled TA for 30 min. Cells were then washed twice with PBS and lysed with 0.1 N NaOH. Accumulation of radiolabeled substrate was determined through scintillation counting. Taurocholate accumulation values in the presence of sodium minus accumulation values in the absence of sodium represented NTCP activity (Anthérieu *et al.*, 2013).

F-actin distribution. After cell exposure to CsA or FK506, cells were washed twice with warm PBS, fixed with 4% paraformaldehyde for 20 min at 4°C and permeabilized with 0.3% Triton in PBS for 30 min. F-actin and nuclei were labeled simultaneously using a phalloidin fluoprobe diluted at 1/100 and 5 ng/ml Hoechst dye, respectively, for 20 min. Imaging was done using the Cellomics ArrayScan VTI HCS Reader (Thermo Scientific) (Anthérieu *et al.*, 2013).

Time-lapse imaging. Phase-contrast images were taken each minute after exposure of HepaRG cells to both immunosuppressant agents, using time-lapse phase-contrast videomicroscopy (Zeiss Axiovert 200M and AxioCam MRm). The inverted microscope was equipped with a thermostatic chamber (temperature and CO_2) to maintain the cells under physiological conditions. Images were captured with a 20× objective and the mosaic tool of the microscope which enabled the automated acquisition of multi-image mosaics at the defined positions.

Measurement of endogenous bile acid content. After treatment of HepaRG cells with CsA for 4 and 24 h both cells and media were collected, lyophilized and stored at −80°C. Ten μl of water was added to 100 mg dried samples, homogenized using a Polytron homogenizer for 30 s, and clarified by centrifugation at 20,000 × g for 20 min. The supernatant was collected and extracted using a solid phase extraction cartridge (SPE). High pressure liquid chromatography coupled with tandem mass spectrometry (HPLC–MS/MS) was used to measure bile acid (BA) content in the samples. The chromatographic separation of BAs was carried out on a Zorbax eclipse XDB-C18 (Agilent Technology, Garches, France) fitted on an Agilent 1100 HPLC system (Massy, France). The column was thermostated at 35°C. The mobile phases consisted of (A) (ammonium acetate 15 mmol/l, pH 5.3) and (B) (methanol) at 65:35 (vol/vol). BAs were eluted by increasing B in A from 65 to 95 (vol/vol) for 30 min. Separation was achieved at a flow rate varying between 0.3 and 0.5 ml/min for 30 min. Mass spectra were obtained using an API 2000 Q-Trap (AB-Sciex, Concord, Ontario, Canada) equipped with a TurboIon electrospray interface set in the negative mode (needle voltage—4500 V) with nitrogen as the nebulizer set at 40 (arbitrary pressure unit given by the equipment provider). Curtain and heater pressures were set at 20 and 40, respectively (arbitrary units), and the ion source temperature was set at 400°C. Declustering and entrance potentials were set at −60 V and −10 V, respectively. The MS/MS detection was operated at unit/unit resolution. The acquisition dwell time for each transition monitored was 70 ms. Data were acquired by the Analyst software (version 1.4.2, AB-Sciex) in the Multiple Reaction Monitoring mode (Humbert *et al.*, 2012).

Western blot analysis of MAPK phosphorylation. Activation of p38-MAPK was assessed by evaluating its phosphorylation status in cell lysates by Western blotting. Briefly, HepaRG cells were incubated with medium alone or with CsA, FK506, and CsA plus inhibitors for 15 or 120 min, washed with cold phosphate-buffered saline, and finally resuspended in cell lysis buffer and a protease inhibitor cocktail. Aliquots containing an equivalent total protein content, as determined by the Bradford procedure with bovine serum albumin as the standard, were subjected to sodium dodecyl sulfate/12% polyacrylamide gel electrophoresis, electrotransferred to Immobilon-P membranes, and probed overnight with a rabbit antiphosphorylated p38 (Cell Signaling Technology, Beverly, MA). After using a mouse anti-rabbit IgG secondary antibody (1:5000, 1 h; ThermoFisher Scientific, Waltham, MA), a chemiluminescence reagent, and Hyperfilm ECL, phosphorylated and total MAPK bands were quantified by densitometry with Fusion-Capt software (Vilber Lourmat, Fusion FX7, France) (Boaglio *et al.*, 2012).

Statistical analysis. The student's *t*-test was applied to compare data between treated and corresponding control cultures. Data were considered as significantly different when $^{*}p < 0.05$, $^{**}p < 0.01$, and $^{***}p < 0.001$.

RESULTS

Cytotoxicity Effects of CsA and FK506

Cytotoxicity of both CsA and FK506 was evaluated in HepaRG cells using the MTT test. CsA did not cause any significant cytotoxicity after 24 h at concentrations up to 100μM. By contrast, FK506 was highly toxic at 100μM causing 94% cell death ($p < 0.001$; Fig. 1A). Based on these data, non-toxic concentrations from 0 to 50μM of both drugs were selected for further studies.

Induction of ROS and ER Stress by CsA

Because deregulation of the cellular redox status is a potent mechanism in DILI, generation of oxidative and ER stress was analyzed after exposure to the two immunosuppressant agents. Significant production of ROS was observed in HepaRG cells

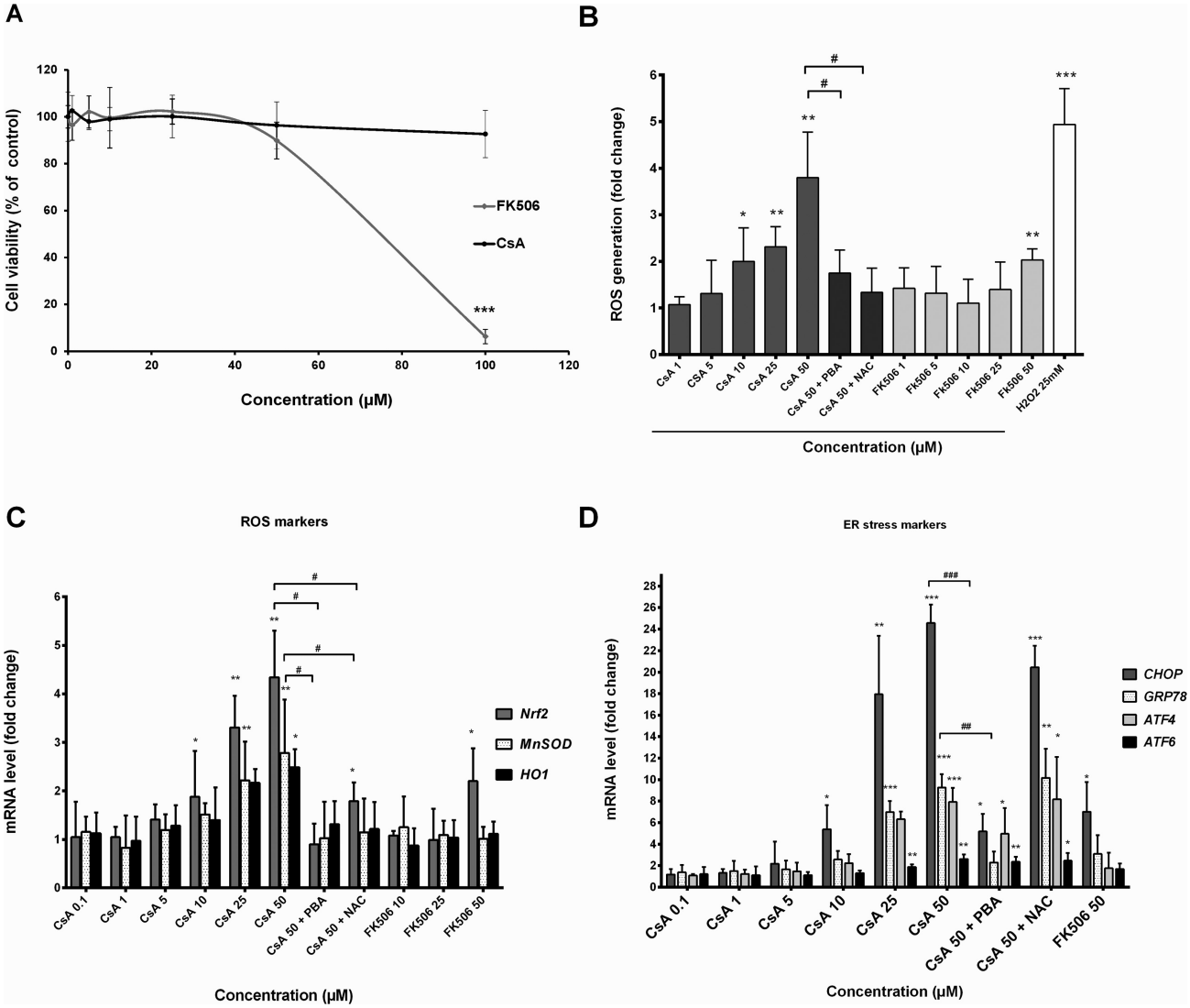

FIG. 1. Cytotoxicity and intracellular generation of ROS in CsA- and FK506-treated HepaRG cells. (A) Cells were incubated for different time points (0–24 h) with different concentrations of either CsA or FK506 (0–100μM). Cytotoxicity was measured by the MTT colorimetric assay. (B) Cells were treated with different concentrations of either CsA or FK506, or co-treated with 50μM CsA + 15mM NAC or 5mM PBA for 2 h. H_2O_2 at 25mM was used as a positive control. ROS generation was detected by the DCFDA specific substrate. (C and D) Cells were treated with CsA or FK506 or co-treated with 50μM CsA + (15mM NAC or 5mM PBA) for 6 h, then mRNA levels of ROS markers (*HO-1*, *MnSOD, and Nrf2*) and ER stress markers (*CHOP*, *GRP78*, *ATF4*, and *ATF6*) were estimated by RT-qPCR. Data represent the means ± SD of three independent experiments. All results are expressed relative to the levels found in untreated cells, arbitrarily set at 1 or 100% $^{*}p < 0.05$, $^{**}p < 0.01$, $^{***}p < 0.001$ compared with non-treated cells, $^{\#}p < 0.05$, $^{\#\#}p < 0.01$, $^{\#\#\#}p < 0.001$ compared with 50μM CsA.

starting at 10μM (twofold; $p < 0.05$) after 2 h (Fig. 1B). ROS formation occurred within the first 15 min after CsA addition (data not shown), peaked after 2 h (3.8-fold; $p < 0.01$) and was totally prevented by co-incubation with 15mM of the antioxidant NAC. Only a slight ROS production was obtained with 50μM FK506 after 2 h (Fig. 1B). Moreover, transcript levels of three ROS markers (*Nrf2*, *HO-1*, *and MnSOD*) were also measured and found to be significantly up-regulated as early as 6 h after CsA exposure (Fig. 1C). Overexpression of *Nrf2* was lower with FK506 and occurring only at 50μM.

Moreover, four ER stress-related genes (*ATF4*, *ATF6*, *GRP78*, and *CHOP*) were strongly up-regulated after 6 h treatment with 50μM CsA, whereas only a slight increase of *CHOP* transcripts was observed with 50μM FK506 (Fig. 1D). Co-treatment with PBA, an ER stress inhibitor, prevented induction of ER stress-related genes. Interestingly, co-treatment with PBA also reduced ROS generation and induction of ROS-related genes, suggesting a link between ER stress and ROS triggered by CsA. However, NAC reduced induction of ROS markers without affecting ER stress-related genes.

In addition, PBA failed to lower ROS induced by H_2O_2 and the cholestatic drug chlorpromazine where no ER stress was observed (Supplementary data 1), indicating that PBA was able to decrease ROS by reducing ER stress, as is the case with high CsA concentrations.

Effects of CsA and FK506 on Influx and Efflux Transporters

CDF and TA substrates were used to evaluate MRP2 and BSEP activity, respectively. To estimate BSEP activity, HepaRG cells were incubated with [^{3}H]-TA for 30 min and then treated for 2 h with either drug in standard buffer containing Ca^{2+}/Mg^{2+}.

A 5-min incubation with Ca^{2+}/Mg^{2+}-free buffer was used to disrupt Ca^{2+}/Mg^{2+}-dependent canalicular tight junctions and eventually evacuate bile canaliculi content; thus only intracellular accumulation of [^{3}H]-TA, which correlated to the effect on canalicular efflux, was measured. In treated cells, CsA inhibited [^{3}H]-TA canalicular efflux in a dose-dependent manner with a 33% ($p < 0.05$) significant inhibition starting at 5μM and reaching 90% ($p < 0.001$) at 50μM (Fig. 2A). On the other hand, 50μM FK506 decreased [^{3}H]-TA canalicular efflux to 58.2% ($p < 0.05$) without any inhibition observed at 10μM (Fig. 2A). To better characterize CsA effects on TA efflux, a time-dependent study was carried out between 0 and 6 h after treatment with 10 and 50μM. Efflux inhibition was evidenced as early as 15 min after CsA addition, whereas its maximum occurred after 2 h. At low CsA concentrations, inhibition was partially restored after 6 h. At higher CsA concentrations inhibition of TA efflux was totally maintained after 6 h (Fig. 2B).

To estimate MRP2 activity, HepaRG cells were exposed to both drugs for 2 h followed by incubation with CDF, an MRP2-specific substrate. CsA inhibited canalicular excretion of CDF at both 10 and 50μM concentrations; no effect was observed with FK506 even at 50μM (Fig. 2C).

The effect of the two immunosuppressant agents on Na^+-dependent BA uptake was estimated through measurement of intracellular accumulation of [^{3}H]-TA after a 30-min incubation. CsA-induced inhibition of NTCP activity started after 30 min with 50μM and 1 h with low doses (≤10μM); it reached a maximum after 2 h and started to be restored after 4 h exposure at low doses, whereas inhibition of [^{3}H]-TA uptake was maintained with 50μM (Fig. 2D). Only a slight inhibition of [^{3}H]-TA uptake was observed with 50μM FK506 after 24 h treatment. Both drugs had no significant effect on Na^+-independent [^{3}H]-TA uptake measured using Na^+-free buffer (data not shown). Further experiments were carried out on progenitors/primitive biliary-like cells after selective enzymatic detachment of hepatocyte-like cells (Cerec *et al.*, 2007) to determine the contribution of these cells in CsA effects. No [^{3}H]-TA uptake was detected (Supplementary data 2), indicating it was exclusively performed by hepatocyte-like cells.

Role of cPKC, ER, and Oxidative Stress in CsA-Induced Effects

It has been demonstrated that cPKC partly accounts for acute cholestasis caused by E17G (Barosso *et al.*, 2012) and that CsA can activate cPKC. We analyzed whether cPKC was involved in CsA-induced cholestatic effects. [^{3}H]-TA efflux was reduced to 21.9% of the control by treatment of HepaRG cells with 10μM CsA for 2 h and was partially restored by co-treatment with the PKC inhibitor H7, rising to 59.4% ($p < 0.05$) of the control (Fig. 3A). Because Ca^{2+} is required for activation of the classical PKCs, we investigated whether Ca^{2+}-mediated activation of these PKC isoenzymes was involved in CsA-induced deleterious effects. Both the intracellular Ca^{2+}-chelator BAPTA/AM and the specific inhibitor of Ca^{2+}-dependent PKCs, Go¨6976, prevented the decrease induced by CsA in [^{3}H]-TA efflux representing 47.4 and 48.7% ($p < 0.01$), respectively, compared with a 21.9% ($p < 0.001$) inhibition with 10μM CsA. When administered alone, none of these inhibitors had any effect on [^{3}H]-TA efflux (data not shown). At high CsA concentration (50μM), none of these inhibitors significantly modulated inhibition of [^{3}H]-TA efflux (Fig. 3A). However, this inhibition was totally restored by co-treatment with either PBA or NAC. Interestingly at low CsA concentrations, co-treatment with PBA has no counteraction effect, favoring a role of ER stress only at high CsA concentrations. By contrast, NAC was totally effective at low and high CsA concentrations indicating a role of ROS in CsA-induced cholestasis whatever the drug concentration (Fig. 3B).

The downstream effector of cPKC, p38, was previously shown to be involved in E17G-cPKC-dependent induced cholestasis (Boaglio *et al.*, 2012). Its specific inhibitor, SB203580, significantly reduced inhibition of [^{3}H]-TA by 10μM CsA to 47.5% ($p < 0.01$) instead of 21.9% ($p < 0.001$) (Fig. 3B). Accordingly, Western blotting analysis of phospho (p)-p38 showed that CsA increased the amount of p-p38 in a time-dependent manner with increment becoming apparent as soon as 5 min after CsA administration. Co-treatment with either the cPKC inhibitor Go¨6976 or NAC selectively prevented p-p38 increase, indicating that p38 activation was dependent on cPKC induction and ROS generation by CsA (Figs. 3C and 3D).

Effects of CsA on BA Disposition

In order to determine whether CsA altered disposition of endogenous BAs, total BA content was quantitated in both media and cells after 4 and 24 h exposure to 10 and 50μM CsA using HPLC–MS/MS. Although no changes were evidenced after 4 h, a concentration-dependent increase of BA content in the medium and decrease in cells was observed after 24 h of CsA treatment. The sum of total BAs content (media + cells) appeared to be nearly unchanged between 4 and 24 h (Fig. 4).

Induction of Cytoskeletal F-Actin Disruption and Bile Canaliculi Constriction by High CsA Concentrations

F-actin cytoskeleton is one of the primary targets of oxidative stress. To determine whether CsA and FK506 disrupted cytoskeletal F-actin distribution, HepaRG cells were exposed to both drugs at different time points and then cytoskeletal F-actin was visualized by phalloidin fluoprobe labeling. Untreated cells showed typical pericanalicular distribution of F-actin and large bile canaliculi with an open lumen (Fig. 5A). At 10μM CsA did not affect actin distribution in the pericanalicular area (Fig. 5B) whereas at 50μM it disrupted its distribution, lowered its labeling intensity, and caused constriction of bile canaliculi after 2-h exposure (Fig. 5D). These effects were confirmed by phase-contrast time-lapse imaging. Retraction and disappearance of bile canaliculi were observed in 50μM CsA-treated cells (Fig. 5G'). FK506 did not alter cytoskeletal F-actin distribution nor bile canaliculi structures (Figs. 5C and 5F').

Effects of CsA and FK506 on Expression of Genes Related to Cholestasis

Many genes involved in BA transport, synthesis, and metabolism are deregulated in cholestasis. A set of target genes was analyzed by RT-qPCR after 24-h treatment with various concentrations of CsA and FK506. These genes included nuclear receptors (*CAR*, *PXR*, *FXR*), efflux transporters (*BCRP*, *BSEP*, *MDR1*, *MDR3*, *MRP2*, *MRP3*, and *MRP4*), uptake transporter *NTCP*, BA metabolism enzymes (*CYP7A1*, *CYP8B1*, and *CYP27A1*), and *CYP3A4*, a BA detoxifying enzyme. At low concentrations up to 10μM CsA slightly induced *PXR*, *FXR*, *CAR*, *NTCP*, *MRP2*, *MRP3*, *MRP4*, *BCRP*, and *CYP3A4* expression whereas at doses >10μM it strongly inhibited most of the tested genes, i.e., *FXR*, *PXR*, *CAR*, *CYP3A4*, *BSEP*, *NTCP*, *MDR1*, *MDR3*, and *CYP8B1*. By contrast, at low concentrations, FK506 was found to induce only *MRP4* and *CYP3A4* whereas at high concentrations it inhibited expression of *PXR*, *CAR*, *BSEP*, *MDR3*, *NTCP*, *CYP27A1*, *CYP8B1*, and *CYP3A4* and induced basolateral transporters (*MRP3*, *MRP4*) as well as *MRP2* and *BCRP* to a similar extent as CsA at the same concentrations (Table 1). No transporter transcripts were detected in progenitors/primitive biliary-like cells when measurements

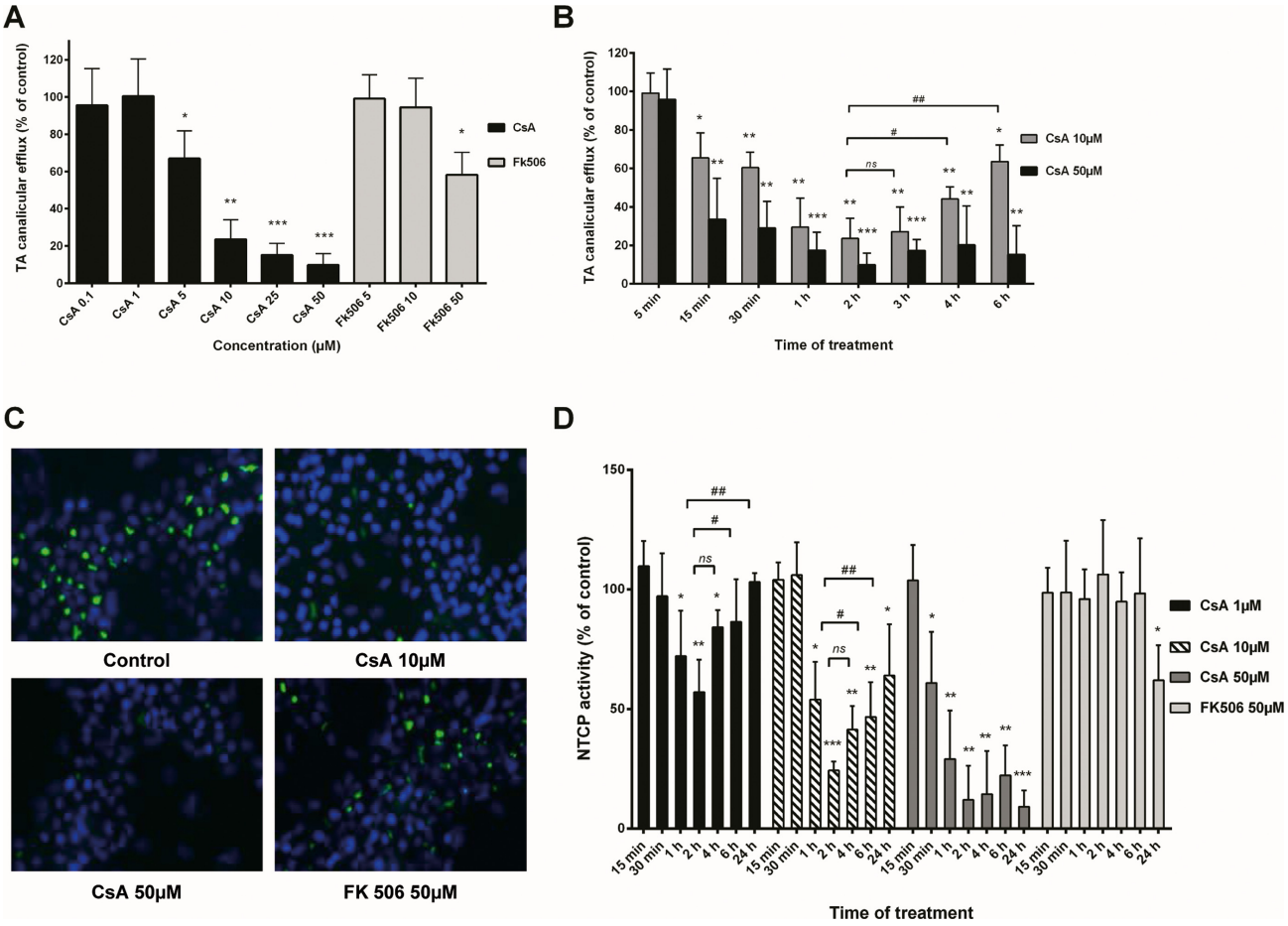

FIG. 2. Effects of CsA and FK506 on activity of efflux transporters. (A and B) Cells were exposed to [^{3}H]-TA in standard buffer for 30 min to induce intracellular accumulation of TA and then incubated with different concentrations of either CsA or FK506 for 2 h (A) or different time points (0–6 h) (B). Bile canaliculi were disrupted by additional 5-min incubation with Ca^{2+}- and Mg^{2+}-free buffer. TA efflux was determined by measuring intracellular TA accumulation. Efflux of TA was expressed relative to the level found in untreated cells, arbitrarily set at a value of 100%. (C) Cells were treated with either CsA or FK506 for 2 h. MRP2 activity was estimated using CDF, a specific substrate; nuclei were stained in blue using Hoechst dye. (D) HepaRG cells were treated with either CsA or FK506 at different concentrations for different time points (0–24 h) and then incubated with [^{3}H]-TA for 30 min. NTCP activity was evaluated by measurement of intracellular accumulation of [^{3}H]–TA. Data represent the means ± SD of three independent experiments. $^*p < 0.05$, $^{**}p < 0.01$, $^{***}p < 0.001$ compared with untreated cells, $^{\#}p < 0.05$, $^{\#\#}p < 0.01$ compared with CsA (same concentration) after 2 h.

were performed after selective detachment of hepatocyte-like cells (not shown).

DISCUSSION

Presently, there is no means for accurate prediction of cholestasis risks in humans; many cholestatic drugs do not induce hepatotoxicity in rats. Using the metabolically competent human HepaRG cells, we demonstrated that CsA induced dose- and time-dependent characteristic features of cholestasis typified by an early inhibition of efflux and uptake of BA and that FK506, another immunosuppressant agent which shares similar immunosuppressive properties and mechanism of action with CsA, was much less cholestatic, inducing some liver disturbances only at high concentrations.

CsA strongly inhibited canalicular efflux of [^{3}H]-TA in a dose-dependent manner in HepaRG hepatocytes, becoming significant at concentrations as low as 5µM after 15 min treatment. This inhibition was reversible at low doses and irreversible at concentrations of 25µM or higher. Recent works using sandwich-cultured primary hepatocytes have well demonstrated that CsA is a powerful inhibitor of BSEP (Pedersen *et al.*, 2013).

CsA also induced a concentration-dependent decrease in NTCP activity measured by Na^+-dependent TA uptake starting after 1 h at low doses (10µM) and even after 30 min at high doses, thereby indicating that inhibition of uptake occurred shortly after efflux inhibition. CsA has been previously shown to decrease uptake of BA in the liver (Murray *et al.*, 2011) but our observation represented the first direct demonstration that inhibition of TA uptake was reversible with low CsA concentrations.

Early effects on efflux and influx of BA by CsA were associated with generation of an oxidative stress and involved deregulation of the cPKC/p38 pathway. A role for oxidative stress as a primary causal agent in induction of drug-induced cholestasis has been reported (Anthérieu *et al.*, 2013; Pérez *et al.*, 2006). Several arguments support the involvement of an oxidative stress in CsA-induced cholestasis, especially ROS generation, and prevention of CsA-induced BSEP activity inhibition and decrease in phospho-p38 protein in the presence of NAC. Compelling evidence that ROS-mediated cholestasis can involve activation of intracellular signaling cascades via cPKC has been provided

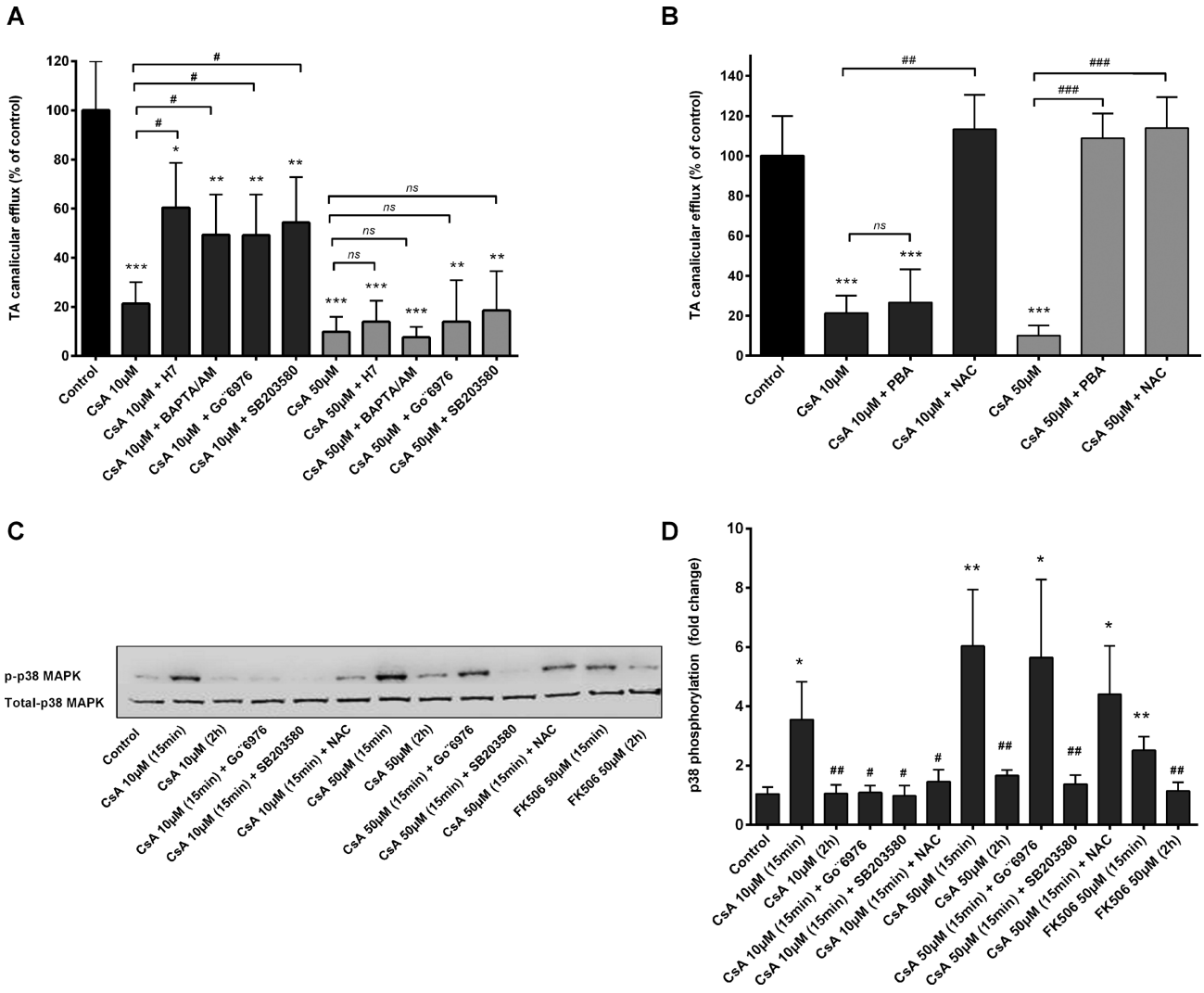

FIG. 3. Effect of Ca^{2+} chelation, cPKC, p38, ER stress, and ROS inhibition on CsA-induced effects. (A) HepaRG cells were exposed to [^{3}H]-TA for 30 min to induce intracellular accumulation of TA and then incubated for 2 h with CsA alone or with either (A) the PKC inhibitor H7 (25µM), cPKC inhibitor Go¨6976 (10µM), p38 inhibitor SB203580 (10µM), or intracellular Ca^{2+} chelator BAPTA/AM (20µM) or (B): 5mM PBA or 15mM NAC. (C) Representative Western blotting of p-p38 and total p38 forms obtained from whole cellular lysates of HepaRG cells incubated with CsA ± inhibitors. (D) Phosphorylation of p38-MAPK quantified as p-p38 to total-p38 ratio. The results are expressed as percentages of untreated cells and are shown as mean ± SD of three independent experiments. $^{*}p < 0.05$, $^{**}p < 0.01$, $^{***}p < 0.001$ compared with untreated cells, $^{\#}p < 0.05$, $^{\#\#}p < 0.01$, $^{\#\#\#}p < 0.001$ compared with CsA alone.

TABLE 1. Effects of CsA and FK506 on Expression of mRNAs Encoding Genes Related to Hepatobiliary Transporters, Nuclear Receptors, and Phase I Metabolizing Enzymes in HepaRG Cells After 24 h Exposure

	CSA 1µM	CSA 5µM	CsA 10µM	CsA 25µM	CsA 50µM	FK506 1µM	FK506 5µM	FK506 10µM	FK506 25µM	FK506 50µM
Nuclear receptors										
FXR	1.27±0.05*	1.18±0.09	1.05±0.18	0.88±0.05	0.69±0.09*	1.045±0.25	1.44±0.33	1.64±0.68	1.173±0.20	0.95±0.21
PXR	1.39±0.1	1.94±0.13***	1.14±0.14	0.44±0.07***	0.32±0.02***	1.07±0.08	1.15±0.09	0.83±0.02	0.94±0.04	0.58±0.12***
CAR	1.4±0.1*	1.25±0.55	1.01±0.30	0.4±0.03***	0.04±0.02***	1.03±0.44	1.44±0.40	0.81±0.21	0.76±0.18**	0.30±0.18**
BA transporters										
BSEP	1.09±0.09	1.01±0.15	0.79±0.17	0.61±0.11**	0.54±0.15**	1.17±0.03	0.76±0.22	0.77±0.14	0.72±0.11*	0.63±0.11**
BCRP	1.19±0.08	2.14±0.11***	2.51±0.50	2.76±0.09***	3.36±0.85*	0.92±0.15	0.95±0.13	0.95±0.13	1.02±0.12	1.74±0.42
MDR3	1.26±0.34	1.161±0.11	0.93±0.17	0.34±0.09***	0.23±0.05***	0.95±0.13	0.89±0.21	0.6±0.15	0.39±0.09**	0.47±0.18*
MRP2	0.9±0.24	1.06±0.21	1.3±0.18*	1.80±0.14***	1.8±0.15***	0.90±0.12	1.35±0.3	1.34±0.28	1.58±0.15*	2.04±0.41*
MRP3	1.02±0.11	1.4±0.18**	1.50±0.14***	1.57±0.07***	1.79±0.08***	1.18±0.13	1.371±0.41	1.41±0.43	1.6±0.23*	1.64±0.32*
MRP4	0.99±0.18	1.44±0.21	1.55±0.18*	2.8±0.09***	2.68±0.12***	1.34±0.17	1.68±0.03***	1.8±0.05***	1.8±0.09*	2.60±0.51*
NTCP	2.16±0.55*	2.64±0.54**	1.51±0.33	0.10±0.02***	0.05±0.01***	1.11±0.24	1.3±0.23	0.82±0.09	0.45±0.15***	0.23±0.08***
BA metabolizing enzymes										
CYP27A1	0.88±0.04	1.04±0.07	0.86±0.03	0.53±0.05***	0.41±0.08***	1.00±0.16	1.16±0.35	0.86±0.11	1.3±0.46	0.47±0.06***
CYP8B1	0.84±0.27	1.15±0.14	0.73±0.24	0.26±0.08	0.05±0.01	1.5±0.25	1.62±0.71	1.03±0.35	0.77±0.08**	0.32±0.1***
CYP7A1	1.08±0.03	1.11±0.07	1.11±0.05	0.92±0.01**	0.42±0.13**	1.06±0.29	1.42±0.37	0.87±0.08	1.4±0.11	0.9±0.12*
CYP3A4	1.62±0.05***	1.51±0.28*	1.33±0.57	0.23±0.05***	0.12±0.01***	1.3±0.23	1.8±0.21**	1.54±0.18*	0.93±0.13	0.34±0.08***

Note: Data represent the means ± SD of three independent experiments. All results are expressed relative to the levels found in untreated cells, arbitrarily set at a value of 1. $^{*}p < 0.05$, $^{**}p < 0.01$, $^{***}p < 0.001$ compared with non-treated cells.

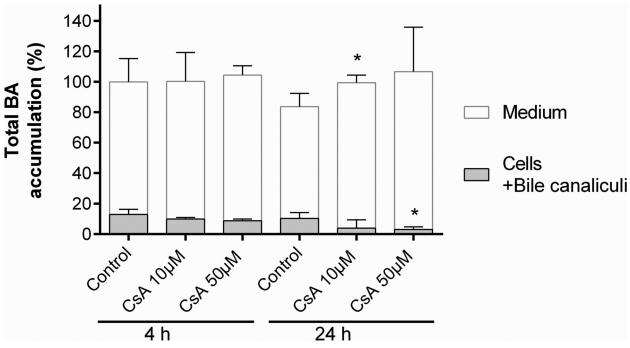

FIG. 4. Effects of CsA treatment on endogenous BAs content. Total BAs were measured in the medium and cells (intracellular + bile canaliculi content) from cultures treated with 10 or 50μM CsA for 4 and 24 h and in corresponding untreated HepaRG cells using LC-MS/MS as described in the Materials and Methods section. Data were normalized relative to the amount of proteins in each condition, and expressed in percentage relative to the total BA content (medium + cells) of untreated cells at 4 h which was arbitrary set at 100. Values represent the sum of means ± SD of duplicate measurements in three independent experiments, $^{*}p < 0.05$ compared with untreated cells. Total BA content (medium + cells) appeared to be nearly unchanged between 4 and 24 h.

(Pérez *et al.*, 2006), and its association with endocytic internalization of BA transporters, such as Mrp2 and Bsep, has been reported (Barosso *et al.*, 2012; Pérez *et al.*, 2006). The downstream effector p38-MAPK has been shown to be differently activated by cPKC isoforms in E17G-induced cholestasis (Boaglio *et al.*, 2012). If cPKC was recently reported to play a major role in CsA toxicity (Sarró *et al.*, 2012), to our knowledge our work is the first to link the sequential activation of cPKC-p38 as a mechanism of CsA-induced cholestasis.

Amplified and irreversible effects of high CsA concentrations on efflux and influx of TA were associated with ROS production and overexpression of ROS markers, *Nrf2, HO-1*, and *MnSOD*, disruption of cytoskeletal pericanalicular F-actin, and constriction of bile canaliculi structures. These effects appeared to be related primarily to induction of an ER stress. Indeed, four major ER stress markers, *ATF4*, *ATF6*, *GRP78*, and *CHOP*, were overexpressed and addition of NAC did not prevent their induction, contrary to PBA, a specific inhibitor of ER stress (Basseri *et al.*, 2009; Carlisle *et al.*, 2014). Obviously, these data support a hierarchical relationship between ER stress and ROS in CsA-induced effects. Contrary to CsA both H_2O_2 (this study) and chlorpromazine (Anthérieu *et al.*, 2013) were able to induce ROS without induction of an ER stress. Moreover, PBA failed to reduce ROS generation by these two molecules (Supplementary data 1), indicating that it cannot reduce ROS unless an ER stress is induced. These data suggest that ER stress might precede an oxidative stress in HepaRG cells treated with high CsA concentrations. This is supported by a recent study on renal proximal tubule cells, which identified ER stress as an early effector of CsA cytotoxicity, leading to ROS generation (Sarró *et al.*, 2012).

The mechanism of CsA-induced ER stress remains poorly studied. A recent proteomic analysis of CsA-treated HepG2 cells has evidenced deregulation of some proteins related to an ER stress without concluding whether it was a primary event in CsA action (Van Summeren *et al.*, 2011). ER stress has been linked to perturbation of cyclophilins A and B distribution in a CsA-treated human kidney cell line (Lamoureux *et al.*, 2011). The relevance between CsA-induced ER and oxidative stress could be related to deregulation of ER-mitochondria Ca^{2+}-signaling bridge. Indeed, ER stress often stimulates a cascade of cellular and molecular events that lead to changes in ER Ca^{2+} concentration resulting in activation of Ca^{2+}-dependent PKC and ROS production (Orrenius *et al.*, 2003). Several arguments support a role of Ca^{2+} in ER and oxidative stress-mediated effects during CsA-induced acute cholestasis, mostly the effectiveness of the Ca^{2+}-chelator BAPTA/AM in reducing CsA cholestatic effects at low concentrations. However, the lack of a Ca^{2+} chelation effect at high CsA concentrations could be explained by the severity and irreversibility of the effects induced by CsA at high doses.

Our data clearly showed that CsA induced ER stress and ROS in HepaRG cells at concentrations which were not cytotoxic whereas FK506 was highly toxic in the absence of ER stress and ROS formation. Accordingly, CsA, but not FK506, was recently reported to induce ER stress in endothelial cells (Bouvier *et al.*, 2009). There is currently no report showing induction of ER stress by FK506 *in vivo*.

Although no obvious change was found in the medium/cells ratio of BAs after a 4-h treatment with 10 or 50μM CsA a concentration-dependent increase in this ratio was observed after 24 h, indicating a cellular (intracellular + bile canaliculi) decrease and not, as it could be expected, an accumulation of BAs. This decrease was not related to a diminution in the content in total BA between 4 and 24 h. These data with CsA as well as those previously obtained with chlorpromazine (Anthérieu *et al.*, 2013) clearly showed that cholestatic features rapidly appeared in HepaRG cells after drug addition; inhibition of BSEP occurred within 1 h and only shortly preceded that of NTCP whereas bile canaliculi constriction was observed within 4 h, giving support to a rapid adaptation of the cells to cholestatic drug effects. The rapid inhibition of the uptake transporter NTCP, bile canaliculi constriction associated with BA discharge, and increased basolateral excretion likely explained the increased medium/cells ratio of BAs after 24 h of CsA treatment. Accordingly, troglitazone, another potent inhibitor of BSEP, failed to induce intracellular accumulation of BAs in human and rat sandwich-cultured hepatocytes, and this result was attributed to compensatory mechanisms which help to maintain BA homeostasis and low intracellular BA concentrations (Marion *et al.*, 2012).

Various cholestasis-related genes were also found to be differently deregulated depending on CsA concentration after a 24-h treatment. At low concentrations the major changes involved overexpression of *PXR, CAR, CYP3A4, NTCP,* and *BCRP*. Although CsA is recognized as a direct inhibitor of *CYP3A4* activity (Amundsen *et al.*, 2012), previous studies have reported induction of *CYP3A4* transcripts by CsA through activation of *PXR* in human primary hepatocytes (Wallace *et al.*, 2010). Because *BCRP* is known to be regulated by *Nrf2*, its overexpression could be related to early *Nrf2* activation by CsA (Singh *et al.*, 2010).

Conversely, overexpression of the basolateral *MRP3* and *MRP4* transporters, and down-regulation of *NTCP*, *CYP27A1*, and *CYP7A1*, the initiator of the BAs biosynthetic pathway, with high CsA concentrations could represent an adaptive defense response aimed at reducing BA accumulation and concomitant toxicity (Zollner and Trauner, 2008).

Compared with CsA, FK506 induced some cholestatic effects only at 50μM, a concentration close to its toxic concentration. Only, *NTCP*, *MRP3*, and *MRP4* were deregulated with 25μM FK506 and to a much lower extent than with 25μM CsA. Moreover, cytoskeletal pericanalicular F-actin and bile canaliculi were not altered. Because FK506 is used at 10- to 100-fold lower doses than CsA, the absence of hepatotoxic and cholestatic effects at concentrations up to 25μM fully agreed with its safety reported in clinics (Mihatsch *et al.*, 1998). Noteworthy, if similar *in vitro* observations as with CsA were recently reported with chlorpromazine

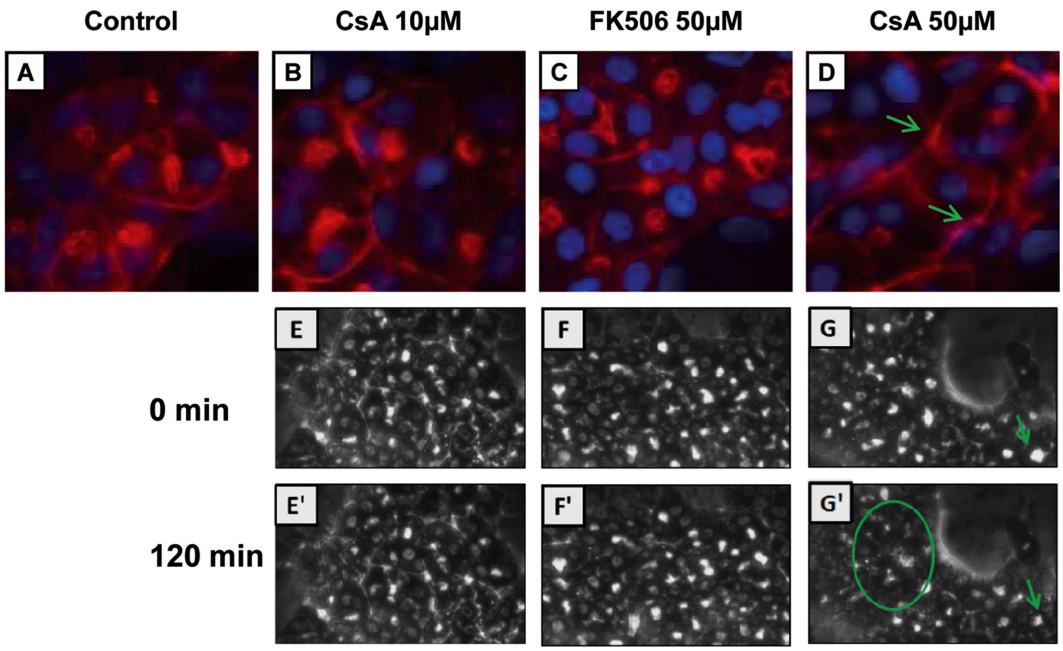

FIG. 5. Alteration of F-actin cytoskeletal distribution and bile canaliculi structures by CsA treatment. (A–D) Untreated cells (A), cells treated with 10μM CsA (B), 50μM FK506 (C), or 50μM CsA (D), after 2 h treatment; F-actin was localized using phalloidin fluroprobe. Nuclei were stained in blue (Hoechst). F-actin shows a predominant pericanalicular distribution around open bile canaliculi in untreated cells and a much less intense staining around constricted bile canaliculi in 50μM CsA-treated cells (arrow). Time-lapse imaging of HepaRG cells treated with 10μM CsA (E'), 50μM FK506 (F'), and 50μM CsA (G') after 120 min compared with corresponding cultures at 0 min (E, F, and G), respectively.

the effects of this idiosyncratic cholestatic drug were, however, observed only at 50μM, a concentration close to its maximum nontoxic concentration (Anthérieu *et al.*, 2013). Accordingly, considering the Cmax values measured in patients, i.e., 1.15, 0.1–0.2, and 0.05μM for CsA, chlorpromazine, and FK506, respectively, cholestatic concentrations are expected to be reached only in patients treated with CsA. These findings suggest that it might be possible to discriminate between dose-dependent and idiosyncratic cholestatic drugs using the HepaRG cell model.

In summary, we demonstrate that reversibility of CsA-induced cholestatic effects is concentration-dependent using HepaRG cells and that ER and oxidative stress are major causal events and involved Ca^{2+}-dependent signaling pathways.

SUPPLEMENTARY DATA

Supplementary data are available online at http://toxsci.oxfordjournals.org/.

FUNDING

European Community [Contracts Predict-IV-202222 and MIP-DILI-115336]. The MIP-DILI project has received support from the Innovative Medicines Initiative Joint Undertaking, resources of which are composed of financial contribution from the European Union's Seventh Framework Programme [FP7/20072013] and EFPIA companies' in kind contribution. http://www.imi.europa.eu/.

Ahmad Sharanek received financial support from the Lebanese Association for Scientific Research (LASeR), Pamela Bachour-El Azzi from Lebanese CNRS and Philippe Jabre Association, and Houssein Al-Attrache from the Association AZM-Lebanese University.

ACKNOWLEDGMENT

We thank Dr. Remy Le Guevel from the ImPACell platform (Biosit, Rennes) for imaging analyses and Dr. Eva Klimcakova for critical reading of the manuscript.

REFERENCES

Amundsen, R., Åsberg, A., Ohm, I. K. and Christensen, H. (2012). Cyclosporine A- and tacrolimus-mediated inhibition of CYP3A4 and CYP3A5 In Vitro. *Drug Metab. Dispos.* **40**, 655–661.

Aninat, C., Piton, A., Glaise, D., Le Charpentier, T., Langouët, S., Morel, F., Guguen-Guillouzo, C. and Guillouzo, A. (2006). Expression of cytochromes P450, conjugating enzymes and nuclear receptors in human hepatoma HepaRG cells. *Drug Metab. Dispos.* **34**, 75–83.

Anthérieu, S., Bachour-El Azzi, P., Dumont, J., Abdel-Razzak, Z., Guguen-Guillouzo, C., Fromenty, B., Robin, M-A. and Guillouzo, A. (2013). Oxidative stress plays a major role in chlorpromazine-induced cholestasis in human HepaRG cells. *Hepatology* **57**, 1518–1529.

Anthérieu, S., Chesné, C., Li, R., Guguen-Guillouzo, C. and Guillouzo, A. (2012). Optimization of the HepaRG cell model for drug metabolism and toxicity studies. *Toxicol. In Vitro* **26**, 1278–1285.

Barosso, I. R., Zucchetti, A. E., Boaglio, A. C., Larocca, M. C., Taborda, D. R., Luquita, M. G., Roma, M. G., Crocenzi, F. A. and Pozzi, E. J. S. (2012). Sequential activation of classic PKC and estrogen receptor α is involved in estradiol 17ß-D-glucuronide-induced cholestasis. *PloS One* **7**, e50711.

Basseri, S., Lhoták, S., Sharma, A. M. and Austin, R. C. (2009). The chemical chaperone 4-phenylbutyrate inhibits adipogenesis by modulating the unfolded protein response. *J. Lipid Res.* **50**,

2486–2501.

Boaglio, A. C., Zucchetti, A. E., Toledo, F. D., Barosso, I. R., Pozzi, E. J. S., Crocenzi, F. A. and Roma, M. G. (2012). ERK1/2 and p38 MAPKs are complementarily involved in estradiol 17ß-D-glucuronide-induced cholestasis: Crosstalk with cPKC and PI3K. *PloS One* **7**, e49255.

Bouvier, N., Flinois, J. P., Gilleron, J., Sauvage, F. L., Legendre, C., Beaune, P., Thervet, E., Anglicheau, D. and Pallet, N. (2009). Cyclosporine triggers endoplasmic reticulum stress in endothelial cells: A role for endothelial phenotypic changes and death. *Am. J. Physiol. Renal Physiol.* **296**, 160–169.

Carlisle, R. E., Brimble, E., Werner, K. E., Cruz, G. L., Ask, K., Ingram, A. J. and Dickhout, J. G. (2014). 4-Phenylbutyrate inhibits tunicamycin-induced acute kidney injury via CHOP/GADD153 repression. *PloS One* **9**, e84663.

Cerec, V., Glaise, D., Garnier, D., Morosan, S., Turlin, B., Drenou, B., Gripon, P., Kremsdorf, D., Guguen-Guillouzo, C. and Corlu, A. (2007). Transdifferentiation of hepatocyte-like cells from the human hepatoma HepaRG cell line through bipotent progenitor. *Hepatology* **45**, 957–967.

Crocenzi, F. A., Mottino, A. D. and Roma, M. G. (2004). Regulation of synthesis and trafficking of canalicular transporters and its alteration in acquired hepatocellular cholestasis. Experimental therapeutic strategies for its prevention. *Curr. Med. Chem.* **11**, 501–524.

Guguen-Guillouzo, C. and Guillouzo, A. (2010). General review on in vitro hepatocyte models and their applications. *Methods Mol. Biol.* **640**, 1–40.

Humbert, L., Maubert, M. A., Wolf, C., Duboc, H., Mahé, M., Farabos, D., Seksik, P., Mallet, J. M., Trugnan, G., Masliah, J. and Rainteau, D. (2012). Bile acid profiling in human biological samples: Comparison of extraction procedures and application to normal and cholestatic patients. *J. Chromatogr. B Analyt. Technol. Biomed. Life Sci.* **899**, 135–145.

Lamoureux, F., Mestre, E., Essig, M., Sauvage, F. L., Marquet, P. and Gastinel, L. N. (2011). Quantitative proteomic analysis of cyclosporine-induced toxicity in a human kidney cell line and comparison with tacrolimus. *J. Proteomics* **75**, 677–694.

Lee, W. M. (2003). Drug-induced hepatotoxicity. *N. Engl. J. Med.* **349**, 474–485.

Marion, T. L., Perry, C. H., St Claire, R. L. and Brouwer, K. L. (2012). Endogenous bile acid disposition in rat and human sandwich-cultured hepatocytes. *Toxicol. Appl. Pharmacol.* **261**, 1–9.

Mihatsch, M. J., Kyo, M., Morozumi, K., Yamaguchi, Y., Nickeleit, V. and Ryffel, B. (1998). The side-effects of ciclosporine-A and tacrolimus. *Clin. Nephrol.* **49**, 356–363.

Mizuta, K., Kobayashi, E., Uchida, H., Fujimura, A., Kawarasaki, H. and Hashizume, K. (1999). Influence of tacrolimus on bile acid and lipid composition in continuously drained bile using a rat model. Comparative study with cyclosporine. *Transpl. Int.* **12**, 316–322.

Murray, J. W., Thosani, A. J., Wang, P. and Wolkoff, A. W. (2011). Heterogeneous accumulation of fluorescent bile acids in primary rat hepatocytes does not correlate with their homogenous expression of ntcp. *Am. J. Physiol. Gastrointest. Liver Physiol.* **301**, 60–68.

Orrenius, S., Zhivotovsky, B. and Nicotera, P. (2003). Regulation of cell death: The calcium-apoptosis link. *Nat. Rev. Mol. Cell Biol.* **4**, 552–565.

Park, B. K., Kitteringham, N. R., Maggs, J. L., Pirmohamed, M. and Williams, D. P. (2005). The role of metabolic activation in drug-induced hepatotoxicity. *Annu. Rev. Pharmacol. Toxicol.* **45**, 177–202.

Pedersen, J. M., Matsson, P., Bergström, C. A., Hoogstraate, J., Norén, A., Lecluyse, E. L. and Artursson, P. (2013). Early identification of clinically relevant drug interactions with the human bile salt export pump (BSEP/ABCB11). *Toxicol. Sci.* **136**, 328–343.

Pérez, L. M., Milkiewicz, P., Elias, E., Coleman, R., Pozzi, E. J. S. and Roma, M. G. (2006). Oxidative stress induces internalization of the bile salt export pump, Bsep, and bile salt secretory failure in isolated rat hepatocyte couplets: A role for protein kinase C and prevention by protein kinase A. *Toxicol. Sci.* **91**, 150–158.

Princen, H. M., Meijer, P., Wolthers, B. G., Vonk, R. J. and Kuipers, F. (1991). Cyclosporin A blocks bile acid synthesis in cultured hepatocytes by specific inhibition of chenodeoxycholic acid synthesis. *Biochem. J.* **275**, 501–505.

Roma, M. G. and Pozzi, E. J. S. (2008). Oxidative stress: A radical way to stop making bile. *Ann. Hepatol.* **7**, 16–33.

Román, I. D. and Coleman, R. (1994). Disruption of canalicular function in isolated rat hepatocyte couplets caused by cyclosporin A. *Biochem. Pharmacol.* **48**, 2181–2188.

Sarró, E., Jacobs-Cachá, C., Itarte, E. and Meseguer, A. (2012). A pharmacologically-based array to identify targets of cyclosporine A-induced toxicity in cultured renal proximal tubule cells. *Toxicol. Appl. Pharmacol.* **258**, 275–287.

Singh, A., Wu, H., Zhang, P., Happel, C., Ma, J. and Biswal, S. (2010). Expression of ABCG2 (BCRP) is regulated by Nrf2 in cancer cells that confers side population and chemoresistance phenotype. *Mol. Cancer Ther.* **9**, 2365–2376.

Stieger, B., Meier, Y. and Meier, P. J. (2007). The bile salt export pump. *Pflugers Arch.* **453**, 611–620.

Tocci, M. J., Matkovich, D. A., Collier, K. A., Kwok, P., Dumont, F., Lin, S., Degudicibus, S., Siekierka, J. J., Chin, J. and Hutchinson, N. I. (1989). The immunosuppressant FK506 selectively inhibits expression of early T cell activation genes. *J. Immunol.* **143**, 718–726.

Van Summeren, A., Renes, J., Bouwman, F. G., Noben, J. P., van Delft, J. H., Kleinjans, J. C. and Mariman, E. C. (2011). Proteomics investigations of drug-induced hepatotoxicity in HepG2 cells. *Toxicol. Sci.* **120**, 109–122.

Wallace, K., Cowie, D. E., Konstantinou, D. K., Hill, S. J., Tjelle, T. E., Axon, A., Koruth, M., White, S. A., Carlsen, H., Mann, D. A., *et al.* (2010). The PXR is a drug target for chronic inflammatory liver disease. *J. Steroid Biochem. Mol. Biol.* **120**, 137–148.

Zollner, G. and Trauner, M. (2008). Mechanisms of cholestasis. *Clin. Liver Dis.* **12**, 1–26.